Research Article | Vol. 33, No. 13 / 30 Jun 2025 / Optics Express 28366
Optics EXPRESS

# Experimental and theoretical study of optical frequency combs in gain-switched Discrete Mode Lasers under optical injection into suppressed longitudinal modes

DANIEL PLAZA-VAS,[1,2,3] MARÍA DUQUE-GIJÓN,[4] CRISTINA MASOLLER,[4] JORDI TIANA-ALSINA,[5] ÁNGEL VALLE,[3] NATHALIE VERMEULEN,[1] AND ANA QUIRCE[1,3,*]

[1]*Brussels Photonics (B-PHOT), Department of Applied Physics and Photonics, Vrije Universiteit Brussel (VUB), Pleinlaan 2, Brussels 1050, Belgium*
[2]*Departamento de Física Moderna, Universidad de Cantabria (UC), Avda. Los Castros s/n, Santander 39005, Spain*
[3]*Instituto de Física de Cantabria (IFCA), Universidad de Cantabria (UC-CSIC), Avda. Los Castros s/n, Santander 39005, Spain*
[4]*Department de Fisica, Universitat Politecnica de Catalunya, Rambla Sant Nebridi 22, 08222 Terrassa, Barcelona, Spain*
[5]*Department de Física Aplicada, Facultat de Física, Universitat de Barcelona, Martí i Franquès 1, 08028 Barcelona, Spain*
[*]*quirce@ifca.unican.es*

**Abstract:** In this work, we investigate how low-power continuous-wave (CW) optical injection into suppressed longitudinal modes far from the free-running mode ($q = 0$) of a single-mode discrete-mode laser (DML) influences the optical frequency combs (OFCs) generated in the DML under gain-switching (GS). In the absence of optical injection, the gain-switched DML emits an OFC at $q = 0$. Optical injection on a distant suppressed mode ($q \neq 0$) produces a second OFC at the injected mode and can also enhance the spectral quality of the $q = 0$ comb. The effects of optical injection depend on injection power and modulation frequency, and different injected modes lead to OFCs with distinct spectral characteristics. The system is frequency tunable over more than 4 THz. These findings demonstrate a novel, robust, and simple approach for generating single- or dual-comb outputs from a GS-DML, offering potential benefits in multiwavelength communications, broadband spectroscopy, and metrology.



## 1. Introduction

Semiconductor lasers are essential for data communication [1,2], spectroscopy [3,4], and quantum photonics applications, such as quantum communications [5]. DMLs achieve single-mode operation by introducing small refractive index perturbations in a Fabry-Pérot (FP) cavity, suppressing undesired longitudinal modes [6,7,8]. DMLs offer several advantages, including narrow linewidth, single-mode emission, reduced sensitivity to optical feedback, and compatibility with photonic integrated platforms in indium phosphide [9] and silicon [10].

OFCs, consisting of equally spaced coherent spectral components, enable a wide range of applications in metrology, spectroscopy, optical sensing [11], high-speed optical communications [12], sub-THz and THz technologies [13,14]. OFCs generated from semiconductor lasers have gained interest for their efficiency, compactness, and low cost [15]. Among various generation techniques, GS stands out for its simplicity, low losses, flexible frequency spacing, and energy efficiency [15]. GS operates by applying a periodic radio-frequency large-signal modulation

#565190 https://doi.org/10.1364/OE.565190
Journal © 2025 Received 16 Apr 2025; revised 2 Jun 2025; accepted 5 Jun 2025; published 26 Jun 2025

Optics EXPRESS

superimposed on the driving current of the laser and is widely employed in multi-carrier communications [16], sub-THz generation [13], and spectroscopy.

CW optical injection, hereafter optical injection, into gain-switched semiconductor lasers enhances OFCs by improving the carrier-to-noise ratio (CNR), reducing linewidth and phase noise, and extending bandwidth [15,17,18]. For multimode FP lasers, optical injection facilitates selective excitation of longitudinal modes, achieving wavelength- tunable OFCs with a range of up to 31 nm in the telecom domain [19]. A different approach [14] injected a narrowband electro-optic comb into the suppressed modes of a chip-integrated multi-wavelength semiconductor laser (MWL). The integration of an optical feedback cavity allowed dynamic control over the feedback phase, enabling nanosecond switching between longitudinal modes, replicating and multiplying the injected comb to achieve THz-scale frequency separations and spectral tunability.

Also, in single-mode gain-switched DMLs, high-power optical injection can lock multiple suppressed longitudinal modes, generating tunable OFCs with a quasi-continuous wavelength range exceeding 37 nm in the telecom domain [20]. In contrast, the present work investigates a fundamentally different regime: low-power optical injection into suppressed modes, well below the locking threshold. Under these conditions, we observe new comb dynamics not addressed in [20], including the simultaneous generation of dual OFCs.

In this experimental and numerical work, we propose a novel, simple, and robust method for generating tunable OFCs by means of low-power CW optical injection into suppressed longitudinal modes, distant from the free-running mode of a single-mode DML under gain switching. In the absence of optical injection, the gain-switched DML emits an OFC centered at its free-running mode. Our approach enables the generation of single- or dual-comb outputs and shows that optical injection into distant suppressed longitudinal modes can also enhance the spectral quality of the free-running comb. The effects of optical injection depend strongly on injection power and modulation frequency, and OFCs with distinct spectral characteristics can be generated depending on the injected mode. In particular, when the DML is gain-switched at a modulation frequency of $f_{mod} = 5$ GHz, low-power optical injection produces a dual-comb output: one at the free-running mode with improved spectral quality, and another at the suppressed injected mode. In contrast, at $f_{mod} = 2$ GHz, a single-comb output is obtained as only a comb is formed at the suppressed injected longitudinal mode.

To support and interpret the experimental results, we also perform numerical simulations based on an extended multimode rate equation model. These simulations reproduce key experimental features and confirm that under suitable modulation and injection conditions, both longitudinal modes can exhibit quasi-deterministic dynamics that enable comb formation. A detailed description of the theoretical model, along with a direct comparison with experimental results, is also provided.

The paper is organized as follows. Section 2 describes the experimental setup. Section 3 presents the experimental results. Section 4 introduces the theoretical model and compares numerical simulations with the experimental data. Finally, Section 5 summarizes the main conclusions.

## 2. Experimental setup

Figure 1 illustrates the all-fiber experimental setup. Light from a tunable laser (Pure Photonics PPCL300), with a narrow linewidth of 75 kHz, is injected into the DML (Eblana Photonics EP1550-0-DM-H19-FM) via an optical circulator. The DC bias current, $I_{bias}$, and the DML temperature are controlled by a laser driver and a temperature controller (Luzwavelabs LDC/E-Current200 and LDC/E-Temp3), respectively. The DML is held at 15 °C and biased at $I_{bias} = 30$ mA, for which the relaxation oscillation frequency is approximately 5.8 GHz. Its threshold current is $I_{th} = 12.3$ mA. Under these conditions, the laser emits approximately 2 mW of optical power.

Optics EXPRESS

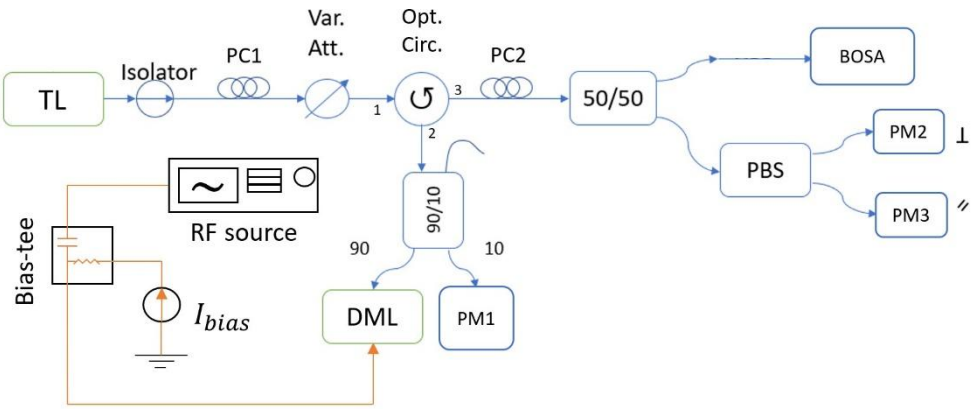


**Fig. 1.** Representation of the all-fiber experimental setup. TL: tunable laser, PC: polarization controller, PM: Power Meter, PBS: polarization beam splitter, DML: discrete mode laser, BOSA: Brillouin optical spectrum analyzer.

The DML is gain-switched by superimposing the DC bias current $I_{bias}$ and a sinusoidal modulation at $f_{mod} = 2$ GHz or 5 GHz via a bias-tee. The modulation signal has a fixed amplitude of $V_{RF} = 1.5$ V and is provided by an RF generator (Keysight N5173B).

An optical isolator is placed after the tunable laser to prevent optical feedback into its cavity. The first polarization controller (PC1) is used to maximize the power injected into the DML. A variable optical attenuator is included to adjust the power level of the externally injected signal. The second port of the optical circulator is connected to a 90/10 fiber coupler; 90% of the light is directed toward the DML, while the remaining 10% is connected to a power meter (PM1) to monitor the injected power ($P_{inj}$).

The DML output exits through the third port of the circulator, passes through a second polarization controller (PC2) and is split by a 50/50 coupler. A polarization beam splitter (PBS) and two power meters are used to optimize the polarization alignment between the tunable laser and the DML, maximizing the injected power. The optical spectrum of the DML is recorded using a high-resolution Brillouin optical spectrum analyzer (BOSA 210, Aragon Photonics) with a resolution of 10 MHz.

The free-running CW DML operates at $\lambda_0 = 1546.025$ nm in a single-mode regime across the entire range of bias currents (14 mA to 90 mA), with adjacent longitudinal modes, suppressed by more than 60 dB and separated by $\delta\lambda$=1.244 nm [20]. The lasing wavelength corresponds to the central longitudinal mode $q = 0$. The optical frequency of the longitudinal mode q of the DML is given by $\nu_q = \nu_0 - q \cdot \delta\nu$, where q is an integer. The corresponding wavelength is $\lambda_q = c/\nu_q$ [20]. When $q = 0$, we have $\nu_0$, which corresponds to the frequency of the longitudinal mode that appears in the free-running DML. Modes with $q > 0$ correspond to longer wavelengths, while those with $q < 0$ indicate shorter wavelengths.

Optical injection is performed at $P_{inj} = 3$ μW and 30 μW targeting specific q-longitudinal modes within a ± 2 THz span around $q = 0$. We examine the effects of modulation frequency ($f_{mod}$) and low injected power ($P_{inj}$). Low-power optical injection is defined as an injection power at least one order of magnitude lower than the power required for injection locking, which typically falls within hundreds of μW [20]. The in-fiber external quantum efficiency is estimated to be $\eta_f \approx 0.17$, consistent with previous results for the same DML device and similar alignment conditions [15].

Optics EXPRESS

## 3. Experimental results

We first show the spectral characteristics of the DML under GS in the absence of optical injection, which we hereafter refer to as the free-running condition. Figure 2 (a) and (b) compare the optical spectra measured at the central mode (q = 0) for modulation frequencies $f_{mod}$ = 5 GHz and $f_{mod}$ = 2 GHz, respectively, both with a modulation amplitude of $V_{RF}$ = 1.5 V. The modulation amplitude $V_{RF}$ = 1.5 V was selected to ensure sufficient modulation depth for comb generation while avoiding excessive carrier depletion at higher modulation frequencies. At $f_{mod}$ = 5 GHz, this amplitude corresponds to a peak-to-peak current swing of approximately 25 mA, based on the system impedance and the estimated radio-frequency cable losses ($C_{loss}$≈0.58). Superimposed on a 30 mA bias current, this results in a total current swing between 5 mA and 55 mA. The modulation frequencies of 2 GHz and 5 GHz were chosen to explore both favorable and unfavorable GS regimes, allowing us to assess how optical injection can enhance or even trigger comb formation depending on the operating conditions. The free-running gain-switched spectra are shown in black, while the CW spectra, i.e., without GS or optical injection, are shown in red for reference. The enhanced comb quality at 5 GHz is attributed to the modulation frequency approaching the laser's relaxation oscillation frequency, a condition known to favor phase-coherent pulse formation and stable comb generation [21].

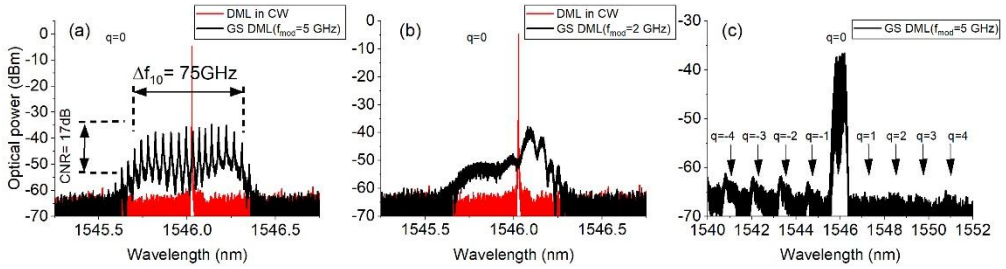


**Fig. 2.** Optical spectrum of the DML operating in CW mode (red curve) and the free-running gain-switched DML (black curve) at $V_{RF}$ =1.5 V and (a) $f_{mod}$ = 5 GHz, (b) $f_{mod}$ = 2 GHz and (c) $f_{mod}$ = 5 GHz, showing the free-running mode (q = 0) and different suppressed longitudinal modes (q≠0).

At $f_{mod}$ = 5 GHz Fig. 2 (a) shows that the gain-switched DML emits an OFC centered at q = 0, with a 5 GHz frequency separation between consecutive lines, a 10 dB spectral width ($\Delta f_{10}$) of 75 GHz, and a CNR of 17 dB. The CNR is calculated as in [22], averaging the intensity of tones within $\Delta f_{10}$ to the noise level between adjacent tones.

In contrast, Fig. 2 (b) illustrates that at $f_{mod}$ = 2 GHz, the optical spectrum of the gain-switched DML at q = 0 becomes broad and noisy, with no well-defined frequencies or evidence of an OFC. Here, the modulation conditions turn the laser off during part of the pulse period, causing pulses to start from spontaneous emission, which disrupts coherence [15].

Moreover, Fig. 2 (c) shows the optical spectrum of the free-running mode (q = 0) and different suppressed longitudinal modes (q≠0) when the DML is gain-switched at $f_{mod}$ = 5 GHz. Notably, carrier density modulation enables the periodic excitation of the suppressed longitudinal modes even in the absence of optical injection. In this free-running state, the q = 0 comb is also reproduced at very low power in the suppressed q < 0 modes, whereas the q > 0 modes remain more strongly suppressed.

Next, we examine the impact of low-power optical injection on the gain-switched DML at $f_{mod}$ = 5 GHz. Figure 3 shows the effect of applying optical injection at $P_{inj}$ = 30 μW into suppressed longitudinal modes q = 4, q = −5, and q = −12. The red arrows indicate the

Optics EXPRESS

wavelengths of the suppressed injected modes, while the blue arrows mark the wavelength of the q = 0 mode.

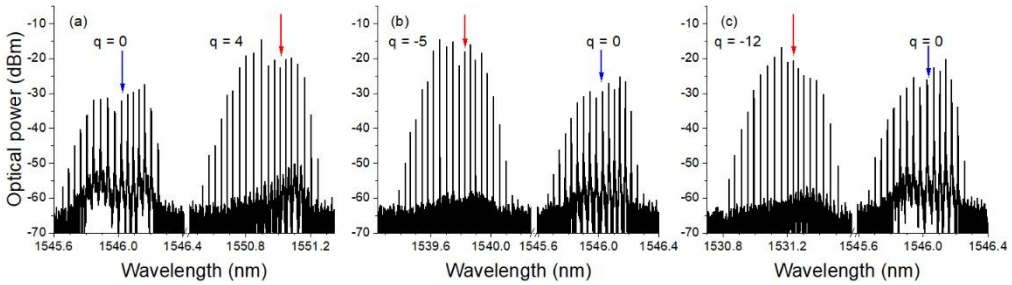


**Fig. 3.** Optical spectra of the gain-switched DML at 5 GHz, $V_{RF} = 1.5$ V and $P_{inj} = 30$ $\mu$W in the longitudinal modes: (a) q = 4 ($\lambda_4$ =1551.017 nm), (b) q = −5 ($\lambda_{-5}$ =1539.830 nm), (c) q = −12 ($\lambda_{-12}$ =1531.240 nm). Red arrows indicate the wavelength at which optical injection is performed. Blue arrows indicate the wavelength of the q = 0 mode.

An important outcome of optical injection under these conditions is the simultaneous generation of a second high-quality OFC at the injected mode q, together with a marked improvement in the spectral characteristics of the free-running q = 0 comb. To facilitate direct comparison, the x-axis is broken to show both OFCs simultaneously. Specifically, the OFC at the injected mode q exhibits a narrower linewidth, reduced noise floor and higher CNR compared to the free-running q = 0 comb shown in Fig. 2(a). At the same time, the q = 0 comb experiences significant enhancements in CNR, linewidth, and noise floor relative to its free-running state.

For optical injection at q = 4 ($\lambda_4$ = 1551.017 nm) Fig. 3(a) illustrates that the injected-mode comb achieves a CNR of 39.1 dB with $\Delta f_{10}$ = 45 GHz. The q = 0 comb improves significantly compared to the free-running case, reaching a CNR of 25.7 dB, with a reduced linewidth and noise floor, although its spectral width decreases to 50 GHz. Injecting further away at q = −5 ($\lambda_{-5}$ = 1539.830 nm) in Fig. 3 (b) leads to even greater enhancements: the OFC at q = −5 achieves a CNR of 45.1 dB, and the q = 0 comb improves to 30.6 dB, both with $\Delta f_{10}$ = 50 GHz and further noise floor suppression compared to Fig. 3(a). These findings indicate a more effective interaction between the injected mode and the free-running mode when optical injection is applied at negative q. Finally, Fig. 3(c) demonstrates the system's tunability with injection at q = −12 ($\lambda_{-12}$ = 1531.240 nm), approximately 15 nm away from q = 0. The OFC at q = −12 reaches a CNR of 40.1 dB with $\Delta f_{10}$ = 45 GHz, while the q = 0 comb maintains a high CNR of 32.1 dB but with a reduced spectral width of 35 GHz, likely due to the larger spectral separation between combs.

These results highlight the robustness of optical injection in generating high-quality dual-OFC emission over a broad spectral range exceeding 4 THz (~2 THz on either side of q = 0). Although the q = 0 comb does not exhibit the same spectral quality as the injected comb, as evidenced in Fig. 3 by the differences in linewidth and noise floor, its spectral characteristics improve significantly under optical injection, even over large spectral separations. As a result, the spectral quality of the q = 0 comb is significantly improved compared to its free-running state (Fig. 2(a)). This behavior is consistent with previous observations in MWLs under modulated optical injection [14].

We then investigate the effect of low-power optical injection when the DML is gain-switched at $f_{mod}$ = 2 GHz, a condition under which free-running operation does not yield an OFC. To carry out the study, we examine two different injection powers. Figure 4 presents the OFCs generated at $P_{inj}$ = 30 μW (Figs. 4(a), 4(c)) and $P_{inj}$ = 3 μW (Figs. 4(b), 4(d)). The injection is applied to the suppressed longitudinal modes q = 4 and q = −12. While optical injection consistently generates

Optics EXPRESS

a high-quality OFC at the injected mode q, it does not significantly enhance the spectrum at q = 0 compared to its free-running spectrum shown in Fig. 2(b). Consequently, Fig. 4 focuses solely on the single OFC obtained at the injected mode.

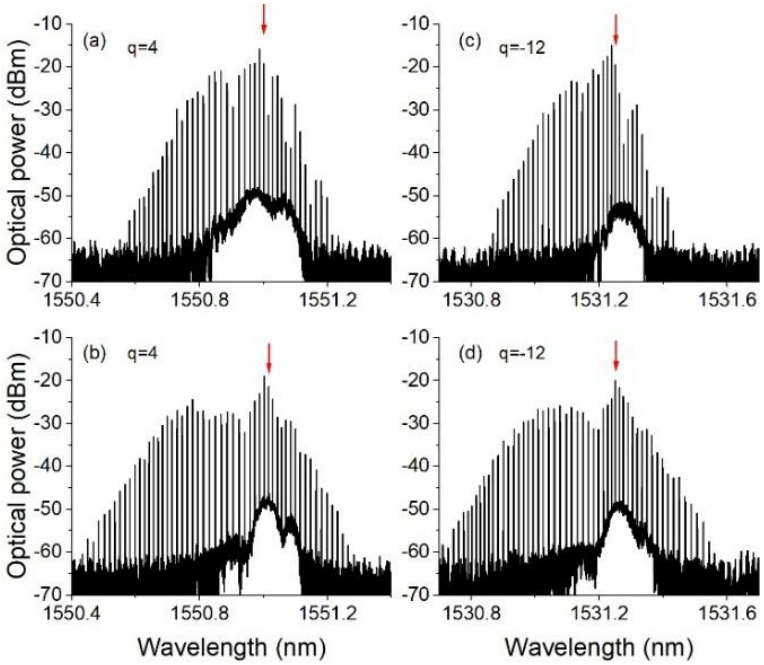


**Fig. 4.** Optical spectra of the gain-switched DML at 2 GHz, $V_{RF} = 1.5$ V, optically injected with $P_{inj} = 30$ μW (a, c) and $P_{inj} = 3$ μW (b, d) in the longitudinal modes: (a, b) q = 4 ($\lambda_4 = 1551.017$ nm), (c, d) q = -12 ($\lambda_{-12} = 1531.240$ nm). Red arrows indicate the wavelength at which optical injection is performed.

Figures 4(a) and 4(b) illustrate the optical spectra for injection at q = 4. At $P_{inj} = 30$ μW, the OFC achieves a CNR of 32.5 dB with $\Delta f_{10} = 30$ GHz. When the injected power is reduced to $P_{inj} = 3$ μW, the CNR decreases slightly to 29.6 dB, while $\Delta f_{10}$ increases to 42 GHz. A similar trend is observed for injection at q = −12. As shown in Figs. 4(c) and 4(d) at $P_{inj} = 30$ μW, the OFC at q = −12 exhibits a CNR of 32.2 dB with a narrow $\Delta f_{10}$ of 18 GHz. Reducing the injected power to $P_{inj} = 3$ μW slightly decreases the CNR to 29.5 dB but significantly broadens $\Delta f_{10}$ to 44 GHz.

These results demonstrate that high-quality, tunable OFC generation over more than 4 THz can be achieved even at extremely low injected power levels (3 μW). This capability persists even at $f_{mod} = 2$ GHz, where the free-running gain-switched DML does not generate a comb (Fig. 2(b)). Furthermore, reducing the injected power consistently broadens the $\Delta f_{10}$, slightly decreases the CNR, and preserves narrow linewidths in the generated OFCs, not only at $f_{mod} = 2$ GHz but also at $f_{mod} = 5$ GHz. For $f_{mod} = 5$ GHz, a high-quality OFC is also obtained at the injected mode q with $P_{inj} = 3$ μW, while maintaining the OFC at q = 0.

To illustrate this behavior, Fig. 5 compares the optical spectra obtained at $P_{inj} = 3$ μW and 30 μW when injecting into the suppressed mode q = −5. Figure 5(a) shows the OFCs at the injected mode q = −5, while Fig. 5(b) displays the corresponding spectra at the free-running mode q = 0. In both cases, the spectra corresponding to $P_{inj} = 3$ μW and 30 μW are superimposed to enable direct comparison at each mode.

Optics EXPRESS

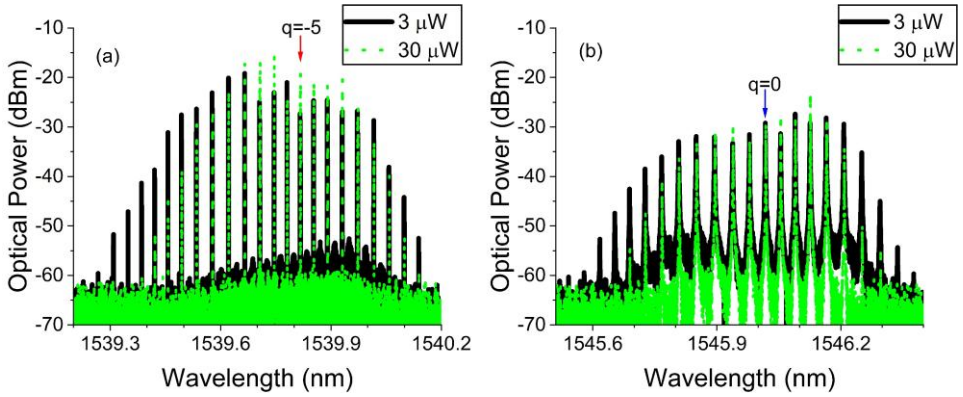


**Fig. 5.** Optical spectra of the gain-switched DML at 5 GHz, $V_{RF}$ = 1.5 V, for two injection powers: $P_{inj}$ = 30 μW (green dashed lines) and $P_{inj}$ = 3 μW (black lines). Optical injection is applied q = −5. (a) Optical spectrum at the injected mode q = −5. (b) Optical spectrum at the non-injected mode q = 0. Red and blue arrows indicate the injection and q = 0 wavelengths, respectively.

The results show that lower injection power leads to slightly broader comb lines and higher noise pedestal levels, particularly at q = 0. At $P_{inj}$ = 30 μW, both combs exhibit narrower lines and lower noise levels. In particular, the non-injected q = 0 comb benefits from a clearer spectral improvement at higher injection power, confirming the role of injection strength in enhancing the spectral characteristics of the generated combs.

These trends were also observed in [15] for the q = 0 mode of a gain-switched DML under optical injection. In that work, the authors demonstrated that as the injected power decreases, injection locking becomes less effective. Consequently, some pulses of the GS-DML lock to the external field while others do not, allowing a larger dynamic chirp during gain switching. This results in a broader 10 dB spectral width and a modest reduction in the CNR, while the individual comb lines remain narrow because the phase coherence between the tunable laser and the DML is still maintained. Although the analysis in [15] focuses solely on the q = 0 mode, we believe that the same underlying physics applies equally to the other longitudinal modes.

Next, we investigate how CNR and $\Delta f_{10}$ depend on q. Figure 6 shows the CNR and the 10 dB spectral width, $\Delta f_{10}$, of the OFCs generated under optical injection with $P_{inj}$ = 30 μW when the DML is gain-switched at $f_{mod}$ = 5 GHz. Results are plotted as a function of the injected longitudinal mode q, ranging from q = −14 to q = 14. Under these conditions, injecting light into any suppressed mode q≠0, results in the simultaneous presence of two OFCs: one at the mode q = 0 and another at the specific injected mode q as illustrated in Fig. 3. The CNR and $\Delta f_{10}$ for the comb at q = 0 are consistently depicted in orange color, while those for the comb at the injected mode, q, are shown in blue color. Solid lines correspond to CNR (left y-axis), and dashed lines represent $\Delta f_{10}$ (right y-axis).

An asymmetry is evident depending on whether the injection is at q > 0 or q < 0, which may stem from the specific design of the DML, where negative modes experience lower optical losses than positive ones (Fig. 2(c)). In [8], also the DML spectrum shows varying power among suppressed longitudinal modes. However, additional device-specific factors, such as variations in the gain spectrum, spatial mode overlap, or fabrication-induced asymmetries, may also play a role and deserve further theoretical and numerical analysis. This suggests that the effectiveness of optical injection may vary when applied to q < 0 modes compared to q > 0 modes. Specifically, the comb at q = 0 and the combs generated at the injected modes q≠0 exhibit higher CNR values when the injection is applied to q < 0 compared to q > 0. Additionally, the CNR of the combs

Optics EXPRESS

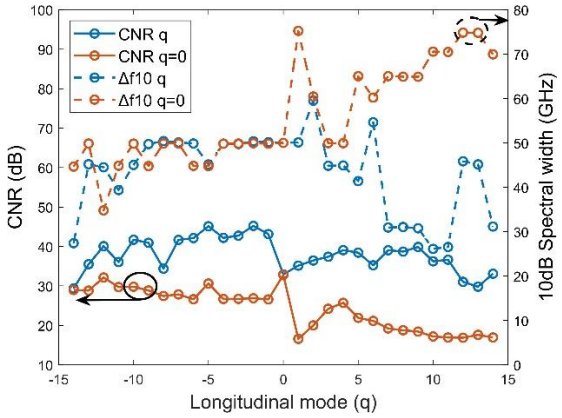


**Fig. 6.** CNR and 10 dB spectral width of the OFCs as a function of the injected mode (q) at $f_{mod} = 5$ GHz, $V_{RF} = 1.5$ V, and $P_{inj} = 30$ μW. Solid and dashed lines represent CNR (left y-axis) and $\Delta f_{10}$ (right y-axis), respectively. Blue corresponds to the values of the comb at the injected mode q, while orange represents the values for the comb at $q = 0$.

at the injected mode $q \neq 0$ consistently exceeds that of the $q = 0$ comb. In the free-running state, the $q = 0$ comb shows a CNR of 17 dB, as shown in Fig. 2(a). Figure 6 demonstrates that optical injection enhances the CNR of the $q = 0$ comb when optical injection occurs at $q \leq 0$ or at $q = 2,3,4,5$ and 6. These enhancements are particularly pronounced when injecting into $q < 0$, indicating a stronger interaction between the optical injection and the $q = 0$ comb. Outside of these cases, the CNR of the $q = 0$ comb does not show significant improvement. In contrast, the CNR of the comb generated at $q \neq 0$ is consistently enhanced compared to the CNR of the free-running $q = 0$ comb mode regardless of the injection mode.

In terms of spectral width, optical injection into any longitudinal mode either reduces or equals the free-running 10 dB spectral width of $\Delta f_{10} = 75$ GHz at $q = 0$. Two behaviors emerge depending on whether the injection is applied to $q < 0$ or $q > 0$. For optical injection into $q < 0$, both the $q = 0$ comb and the q comb evolve to $\Delta f_{10} \sim 50$ GHz, below the free-running value. In contrast, when optical injection occurs at $q > 0$, the $\Delta f_{10}$ of the $q = 0$ comb can increase with increasing q, but generally remains below the free-running $\Delta f_{10}$ except at $q = 1,13$, and 14 where it recovers to ~75 GHz. Moreover, any increase in $\Delta f_{10}$ for $q > 4$ comes at the cost of reduced CNR, highlighting a trade-off between spectral width and CNR. However, this $\Delta f_{10}$ increase does not occur for the positive q injected modes themselves, which tend to exhibit narrower spectral widths, always below the free-running 75 GHz and also below the ~50 GHz characteristic of the negative q injection case.

When injection is performed directly into the $q = 0$ mode, Fig. 6 shows a substantial increase in the CNR compared to the 17 dB CNR in free-running operation, but no improvement in $\Delta f_{10}$, which remains around 50 GHz.

The results reveal that injecting into suppressed longitudinal modes, even when far from $q = 0$, leads to a notable improvement in the CNR of the $q = 0$ comb. However, this improvement is smaller than the CNR obtained at the q injected mode, and this process does not enhance the 10 dB spectral width of the free-running $q = 0$ comb. Furthermore, the results confirm that optical injection can generate two tunable OFCs: one at $q = 0$ and another at the injected mode q, both exhibiting good CNR and moderate $\Delta f_{10}$. These OFCs span a range exceeding 2 THz on either side of $q = 0$, limited in our case by the spectral measurement range of the optical spectrum analyzer.

Optics EXPRESS

## 4. Theoretical results

We now show the theoretical model that we have used for describing the dynamics of a semiconductor laser emitting in two longitudinal modes, q = 0 and q≠0. This is a rate equations model for the complex electric field associated to both modes, $E_0(t)=E_{01}(t)+iE_{02}(t)$ and $E_q(t)=E_{q1}(t)+iE_{q2}(t)$ for the 0 and q-mode, respectively. These equations are based on the models explained in [15,23], extended to account for a second longitudinal mode with different optical losses, and to account for the effect of external optical injection too. The equations read

$$\frac{dE_0}{dt} = \left[\left(\frac{1}{1+\varepsilon\left(|E_0|^2+|E_q|^2\right)}+i\alpha\right)G_N(N-N_t)-\frac{1+i\alpha}{\tau_p}\right]\frac{E_0}{2} + iq\pi\delta\nu E_0 + \gamma_a E_0 + \frac{E_{inj}}{\tau_p}e^{i2\pi\Delta\nu t} + \sqrt{\frac{\beta B}{2}}N\xi_0(t) \tag{1}$$

$$\frac{dE_q}{dt} = \left[\left(\frac{1}{1+\varepsilon\left(|E_0|^2+|E_q|^2\right)}+i\alpha\right)G_N(N-N_t)-\frac{1+i\alpha}{\tau_p}\right]\frac{E_q}{2} - iq\pi\delta\nu E_q - \gamma_a E_q + \frac{E_{inj}}{\tau_p}e^{i2\pi\Delta\nu t} + \sqrt{\frac{\beta B}{2}}N\xi_q(t) \tag{2}$$

$$\frac{dN}{dt} = \frac{I(t)}{e} - \left(AN+BN^2+CN^3\right) - \frac{G_N(N-N_t)\left(|E_0|^2+|E_q|^2\right)}{1+\varepsilon\left(|E_0|^2+|E_q|^2\right)} \tag{3}$$

where *N(t)* is the number of carriers in the active region and *I(t)* is the injected current given by

$$I(t) = I_{bias} + C_{loss}\,(f_{mod})\frac{2\sqrt{2}V_{RF}}{Z_0+Z_L}\sin(2\pi f_{mod}t). \tag{4}$$

The meaning of the parameters and their numerical values are the following: $G_N$, differential gain ($1.48\cdot10^4$ $s^{-1}$); $N_t$, carrier number at transparency ($1.93\cdot10^7$); $\alpha$, linewidth enhancement factor (3); $\varepsilon$, non-linear gain coefficient ($7.73\cdot10^{-8}$); $\tau_p$, photon lifetime (2.17 ps); $\delta\nu$, free spectral range (140 GHz); $2\gamma_a$, difference in losses between the longitudinal modes (1.4 $ns^{-1}$); $\beta$, fraction of spontaneous emission coupled into the lasing mode ($5.3\cdot10^{-6}$); $A$, non-radiative recombination coefficient ($2.8\cdot10^8$ $s^{-1}$); $B$ spontaneous recombination parameter (9.8 $s^{-1}$); $C$, Auger coefficient ($3.84\cdot10^{-7}$ $s^{-1}$); $E_{inj}$, amplitude of the field of the injected light (0.2); Δν, frequency detuning of the optical injection with respect to the zero frequency, that corresponds to the middle optical frequency between those of the q = 0 and q≠0 modes (71.4 GHz), $C_{loss}(f_{mod})$, loss coefficient accounting for the frequency dependent electrical cable attenuation (0.58), $Z_0$ is the generator output impedance (50 Ω), and $Z_L$ is the impedance of the laser module (50 Ω). The Langevin terms, $\xi_0$ and $\xi_q$, represent fluctuations due to spontaneous emission that are assumed to be independent with the following correlation properties, $\langle\xi_0(t)\xi_0^*(t')\rangle=2\delta(t-t')$, and $\langle\xi_q(t)\xi_q^*(t')\rangle=2\delta(t-t')$.

We perform the numerical integration of the Eqs. (1)-(3) by using the Euler-Maruyama algorithm with an integration time step of 0.001 ps. Figure 7 shows the numerical results obtained when considering the q = 0, and q = −1 modes, with $I_{bias}$ = 30 mA, $f_{mod}$ = 5 GHz, and $V_{RF}$ = 1.5 V. Figure 7(a) shows the optical spectrum obtained by averaging the fast Fourier transform of the optical field over 200 windows of 81.92 ns duration each, with a 1.25 ps sampling time. The numerical spectrum shows similar characteristics to those observed in Fig. 3. Also, we can

Optics EXPRESS

compare with the experimental spectrum that corresponds to optical injection at q = −1 mode, that is shown in Fig. 8. Two high-quality OFCs appear at q = −1 and q = 0 modes, both in Fig. 7(a) and in Fig. 8. This can be explained by plotting the temporal evolution of the photon number emitted in each longitudinal mode, $|E_0|^2$ and $|E_{-1}|^2$. Figure 7(b) shows that evolution for q = 0 and q = −1 modes in vertical logarithmic scale. This figure shows that under the considered modulation conditions the minimum photon number in both modes is around 100, a value much larger than the values that should be expected if the power decreases to levels dominated by spontaneous emission noise. For instance, if $V_{RF}$ increases to 3 V, the minimum values of the photon number are between 3 and 4 orders of magnitude smaller than in Fig. 7(b). The almost deterministic evolution of the photon number results in a rather deterministic evolution of the optical phase with the corresponding formation of the OFCs shown in Fig. 7(a). A systematic theoretical analysis of optical frequency comb formation will be the subject of future work. Comparison between Fig. 7(a) and Fig. 8 shows that there is a good agreement between our experimental results and the theoretical results obtained with a model in which the parameters have been extracted for our device [17,24].

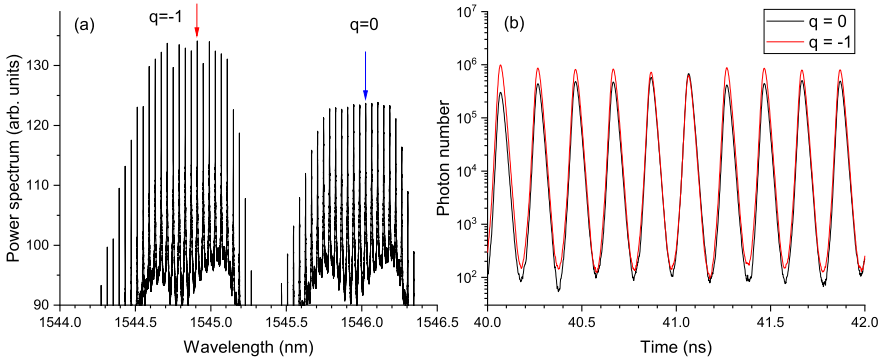


**Fig. 7.** (a) Theoretical optical spectrum of the gain-switched DML emitting in the q = 0 and q = −1 longitudinal modes. The red arrow indicates the wavelength at which optical injection is performed and the blue arrow indicates the wavelength of the q = 0 mode. (b) Photon number in each of the longitudinal modes.

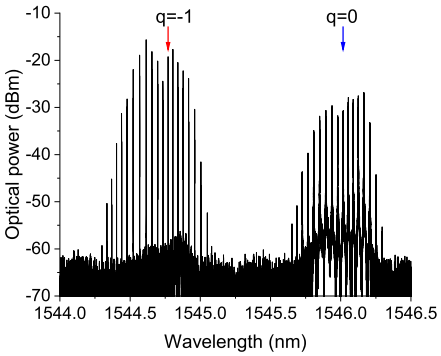


**Fig. 8.** Experimental optical spectrum of the gain-switched DML at 5 GHz, $V_{RF}$ = 1.5 V, and $P_{inj}$ = 30 μW. Optical injection is applied at q = −1. The red arrow indicates the wavelength at which optical injection is performed and the blue arrow indicates the wavelength of the q = 0 mode.

Optics EXPRESS

## 5. Summary and conclusions

Summarizing, we have shown that low-power optical injection into suppressed longitudinal modes of a gain-switched single-mode DML enables the generation of tunable OFCs. Optical injection at a distant suppressed mode, q≠0, can activate a high-quality OFC at the injected mode while simultaneously enhancing the spectral quality of the comb at the fundamental mode, q = 0, leading to two simultaneous OFCs. The effects of optical injection depend on injection power and modulation frequency, influencing the spectral properties of the generated combs. Despite this dependence, the system remains tunable over more than 4 THz, demonstrating a robust approach for generating single- or dual-comb outputs from a GS-DML. The asymmetry between injections at negative and positive q, suggests that device-specific losses or cavity design features could enhance comb performance. These findings hold promise for multiwavelength communications and broadband spectroscopy.

**Funding.** Ministerio de Ciencia, Innovación y Universidades (PID2021-123459OB-C22MCIN/AEI/FEDER, UE, CNS2023-143986MICIU/AEI/NextGenerationEU/PRTR); Fonds Wetenschappelijk Onderzoek (G005420N); Vrije Universiteit Brussel-OZR; Agència de Gestió d'Ajuts Universitaris i de Recerca (2021 SGR 00606, FI scholarship); Institució Catalana de Recerca i Estudis Avançats.

**Acknowledgment.** D. Plaza-Vas and N. Vermeulen acknowledge financial support from FWO, Belgium under Grant G005420N and from VUB-OZR, Belgium. M. Duque, J. Tiana, C. Masoller acknowledge financial support from AGAUR (2021 SGR 00606 and FI scholarship), ICREA Academia.

**Disclosures.** The authors declare no conflicts of interest.

**Data availability.** Data will be made available upon reasonable request.

## References

1. J. Pfeifle, V. Vujicic, R. T. Watts, *et al.*, "Flexible terabit/s Nyquist-WDM super-channels using a gain-switched comb source," Opt. Express **23**(2), 724–738 (2015).
2. C. Browning, H. H. Elwan, E. P. Martin, *et al.*, "Gain-Switched Optical Frequency Combs for Future Mobile Radio-Over-Fiber Millimeter-Wave Systems," J. Lightwave Technol. **36**(19), 4602–4610 (2018).
3. B. Jerez, P. Martín-Mateos, E. Prior, *et al.*, "Dual optical frequency comb architecture with capabilities from visible to mid-infrared," Opt. Express **24**(13), 14986–14994 (2016).
4. C. Quevedo-Galán, V. Durán, A. Rosado, *et al.*, "Gain-switched semiconductor lasers with pulsed excitation and optical injection for dual-comb spectroscopy," Opt. Express **28**(22), 33307–33317 (2020).
5. T. K. Paraïso, R. I. Woodward, D. G. Marangon, *et al.*, "Advanced laser technology for quantum communications (tutorial review)," Adv. Quantum Technol. **4**(10), 2100062 (2021).
6. B. Corbett and D. McDonald, "Singe longitudinal mode ridge waveguide 1.3 nm Fabry-Perot laser by modal perturbation," Electron. Lett. **31**(25), 2181–2182 (1995).
7. S. Osborne, S. O'Brien, K. Buckley, *et al.*, "Design of Single-Mode and Two-Color Fabry-Pérot Lasers With Patterned Refractive Index," IEEE J. Sel. Top. Quantum Electron. **13**(5), 1157–1163 (2007).
8. C. Herbert, D. Jones, A. Kaszubowska-Anandarajah, *et al.*, "Discrete mode lasers for communication applications," IET Optoelectron. **3**(1), 1–17 (2009).
9. P. M. Anandarajah, S. Latkowski, C. Browning, *et al.*, "Integrated Two-Section Discrete Mode Laser," IEEE Photonics J. **4**(6), 2085–2094 (2012).
10. J. Huang, W. Wei, B. Yang, *et al.*, "Monolithic Quantum Dot Discrete Mode Laser on SOI," ACS Photonics **10**(6), 1813–1820 (2023).
11. T. Fortier and E. Baumann, "20 years of developments in optical frequency comb technology and applications," Commun. Phys. **2**(1), 153 (2019).
12. M. Imran, P. M. Anandarajah, A. Kaszubowska-Anandarajah, *et al.*, "A Survey of Optical Carrier Generation Techniques for Terabit Capacity Elastic Optical Networks," IEEE Commun. Surv. Tutorials **20**(1), 211–263 (2018).
13. Á. R. Criado, C. de Dios, E. Prior, *et al.*, "Continuous-Wave Sub-THz Photonic Generation With Ultra-Narrow Linewidth, Ultra-High Resolution, Full Frequency Range Coverage and High Long-Term Frequency Stability," IEEE Trans. Terahertz Sci. Technol. **3**(4), 461–471 (2013).
14. S. Abdollahi, M. Ladouce, P. Marin-Palomo, *et al.*, "Agile THz-range spectral multiplication of frequency combs using a multi-wavelength laser," Nat Commun **10** 1305 (2024).
15. A. Rosado, A. Pérez-Serrano, J. M. G. Tijero, *et al.*, "Numerical and experimental analysis of optical frequency comb generation in gain-switched semiconductor lasers," IEEE J. Quantum Electron. **55**(6), 1–12 (2019).
16. P. Anandarajah, R. Maher, Y. Xu, *et al.*, "Generation of coherent multicarrier signals by gain switching of Discrete Mode Lasers," IEEE Photonics J. **3**(1), 112–122 (2011).
17. A. Quirce, A. Rosado, J. Díez, *et al.*, "Nonlinear dynamics induced by optical injection in optical frequency combs generated by gain-switching of laser diodes," IEEE Photonics J. **12**(4), 1–14 (2020).

Optics EXPRESS

18. S. P. Ó Dúill, P. M. Anandarajah, R. Zhou, *et al.*, "Numerical investigation into the injection-locking phenomena of gain switched lasers for optical frequency comb generation," Appl. Phys. Lett. **106**(21), 211105 (2015).
19. G. Jain, D. Gutierrez-Pascual, M. J. Wallace, *et al.*, "Experimental investigation of external optical injection and its application in gain-switched wavelength tunable optical frequency comb generation," J. Lightwave Technol. **39**(18), 5884–5895 (2021).
20. A. Quirce, B. Kelleher, and A. Valle, "Optical Injection Locking of Longitudinal Modes in a Discrete Mode Laser: Application in Gain-Switched Optical Frequency Combs," J. Lightwave Technol. **42**(10), 3799–3806 (2024).
21. P. M. Anandarajah, S. P. Ó Dúill, R. Zhou, *et al.*, "Enhanced Optical Comb Generation by Gain-Switching a Single-Mode Semiconductor Laser Close to Its Relaxation Oscillation Frequency," IEEE J. Select. Topics Quantum Electron. **21**(6), 592–600 (2015).
22. A. Rosado, A. Pérez-Serrano, J. M. G. Tijero, *et al.*, "Experimental study of optical frequency comb generation in gain-switched semiconductor lasers," Opt. Laser Technol. **108**, 542–550 (2018).
23. A. Valle, "Divergence of the variance of the optical phase in gain-switched semiconductor lasers described by stochastic rate equations," Phys. Rev. Appl. **19**(5), 054005 (2023).
24. A. Quirce and A. Valle, "Spontaneous emission rate and phase diffusion in gain-switched laser diodes," Opt. Laser Technol. **150**, 107992 (2022).